A CFD Assessment of Several High-Lift Reference H Configurations Using Structured Grids

Aerodynamic Performance Workshop
February 25-28, 1997

Wendy B. Lessard
NASA LaRC

HSR H-L CFD

Objective

Solve the viscous subsonic flowfield for the high-lift RefH configuration and determine the ability of an existing structured Navier-Stokes code to accurately predict this flow

Outline

- Grids
- Flow solver
- Results
  - Convergence and resources used
  - Force and moment comparisons
  - Pressure data correlations
  - Off-surface and surface flow viz
- Conclusions

HSR H-L CFD

The objective of this study is to calibrate a Navier-Stokes code for a high-lift Reference H configuration using structured grids.

The outline of this presentation will first include a brief description of the grids used and the flow solver. Next the results will be presented in terms of convergence and resources used on the C-90. Predicted force and moment and surface pressure results are compared to experiment and off- and on-surface flow viz is discussed.

Concluding remarks follow.

GRIDS

Three grids were generated of the high-lift ($\delta_{LE} = 30^\circ$ / $\delta_{TE} = 10^\circ$)
Reference H config by Langley's Geometry Lab

Geometry	Blocks	Grid Pts	Patched	Pt-Pt
w/b	14	3,988,514	2	23
w/b/n/ht	37	4,595,343	38	83
w/b/n/emp	74	7,085,708	96	163

HSR H-L CFD

GEOLAB generated three RefH high-lift configurations, which are shown in the table. The leading- and trailing-edge flaps were deflected 30° and 10°, respectively. (All the leading-edge flaps were down). The full-span configuration was generated for side-slip calculations, and this grid was actually a coarsened version of config2 (with the vertical tail attached) and mirrored to the other side.

Reference H Grid Topology

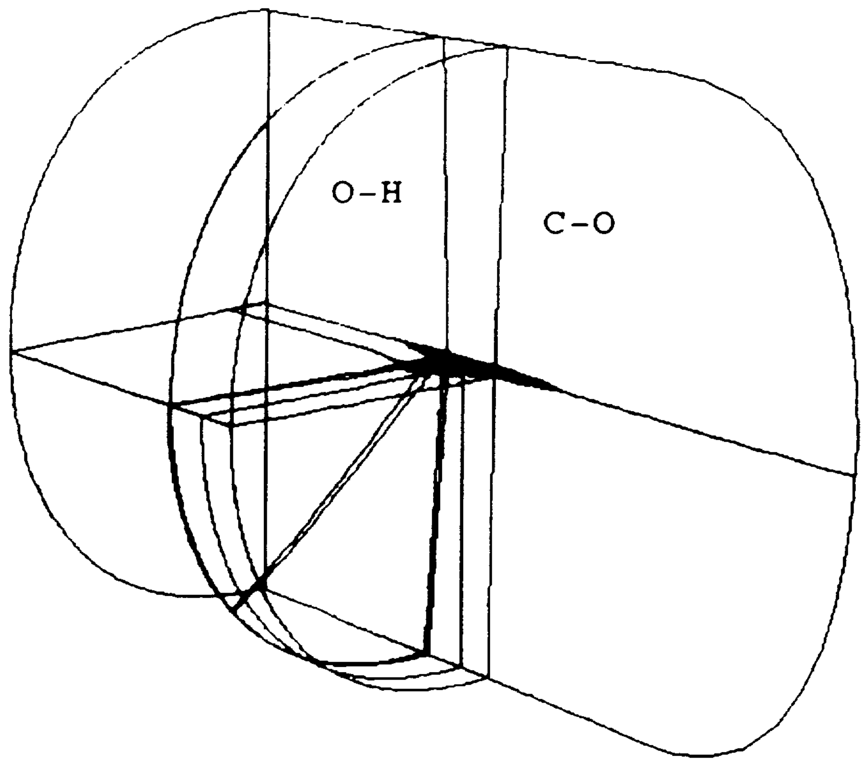

This figure shows the outline of the multi-block grid which was used for all the grids. The basic gridding topology was C-O for the forebody and O-H for the wing/fuselage and aftbody.

Reference H Block Details Around Trailing-Edge Flaps and Nacelles

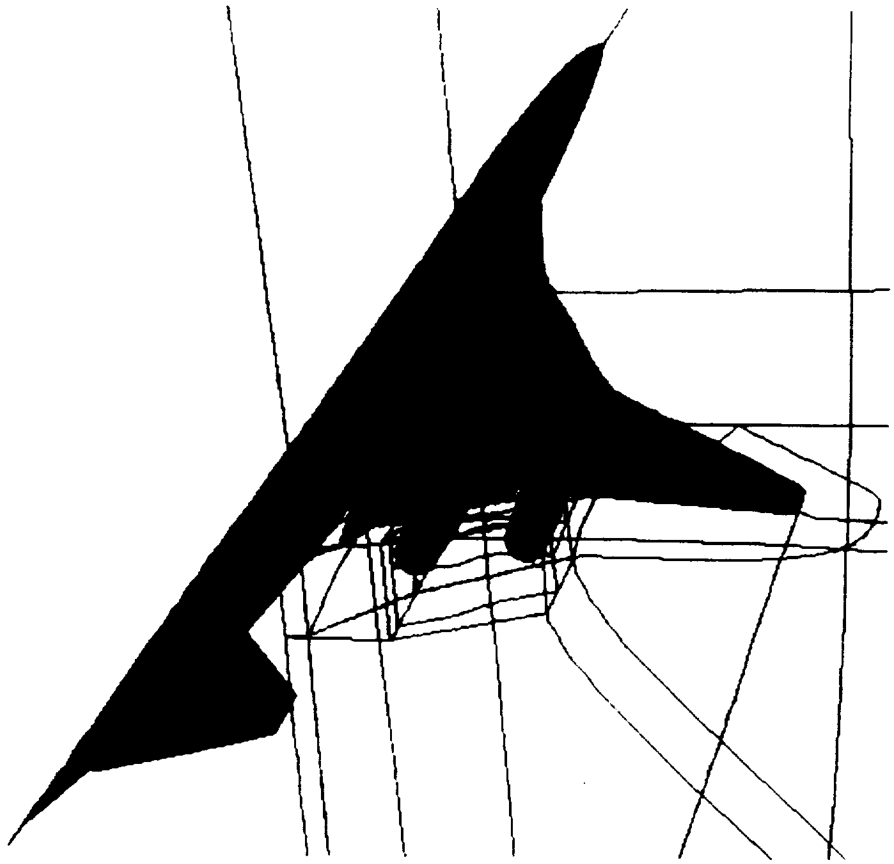

A close-up view of the high-lift RefH grid is shown in this figure, which details the complex blocking structure around the nacelles. An additional 23 blocks were added to the wing/body case in order to model the nacelles.

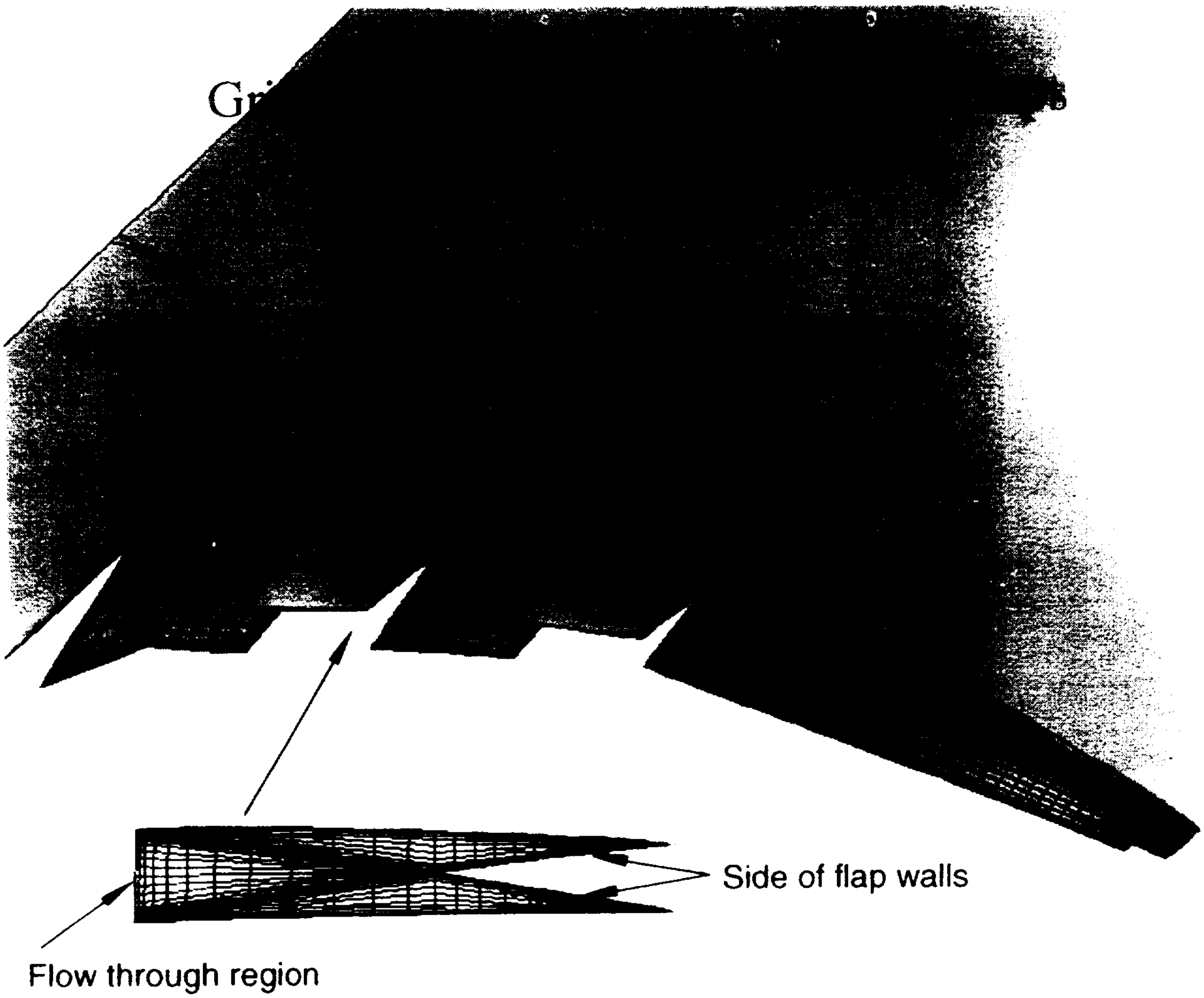

This figure highlights the surface grids on the RefH trailing-edge flaps and the gridding strategy used to model the sides of the flap regions. As shown in the insert, two small triangular grids were generated which model the sides of the flap walls. And the middle triangular region simulated flow through, which maintained point-to-point matching across the interface.

CFL3D

- Solves the time-dependent Reynolds-averaged Navier-Stokes equations on structured grids.
- Multigrid and mesh sequencing for convergence acceleration.
- Baldwin-Lomax with Degani-Schiff turbulence model.
- Multitasked for use on several processors with an average speed-up time of 1.5.

HSR H-L CFD

The slide is self-explanatory

RESOURCE REQUIREMENTS

All cases were run on the C-90 at NAS

Alias	RefhH Geom	Cases	Memory	Avg Run
config1	w/b	α=6,8,10,12,15	170 mw	15 hrs
config2	w/b/nac/htail	α=8,10,12	180 mw	18 hrs
config3	w/b/nac/emp full-span	α=8 β=0,6,12,18	260 mw	25 hrs

HSR H-L CFD

The resource requirements using CFL3D on the C-90 at NAS are shown in the following table, which summarizes the memory required and the average run time for all the cases considered.

Convergence Characteristics for H-L Reference H, w/b/n/htail at $\alpha = 10°$
M = 0.24, Re = 8 mil

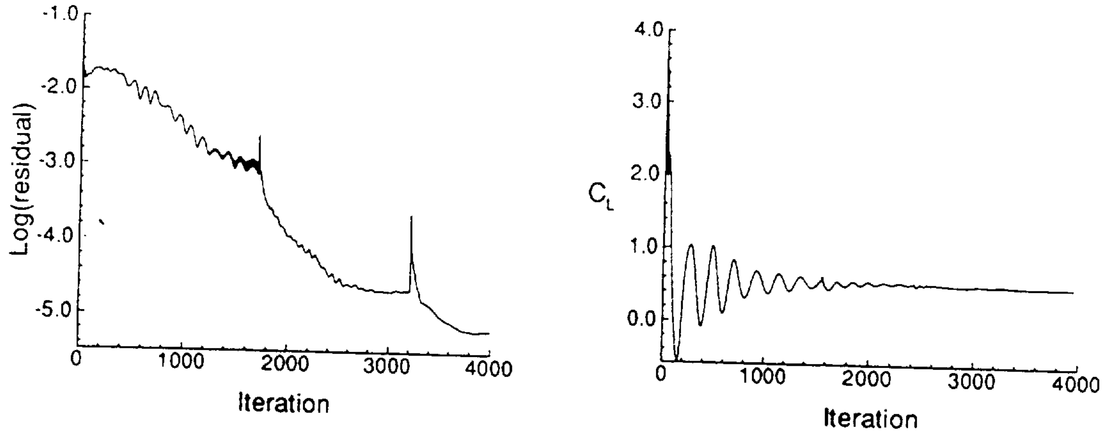

Convergence Characteristics for H-L Reference H, w/b/n/emp at $\alpha = 8°$, $\beta = 12°$

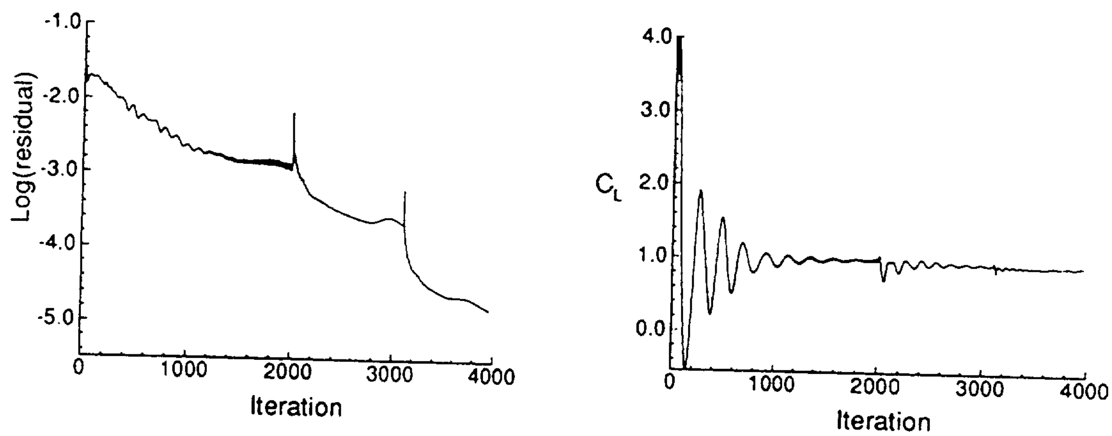

Residual and lift histories for the config2 case at $\alpha = 10°$ and the full-span config3 case at $\alpha = 8°$ and $\beta = 12°$, $M = 0.24$ and $Re = 8.0$ million. Both show approximately 3.5 order reduction in residual magnitude with negligible oscillations in C_L

Forces and Moments for Reference H w/b

M = 0.24, Re = 8 mil

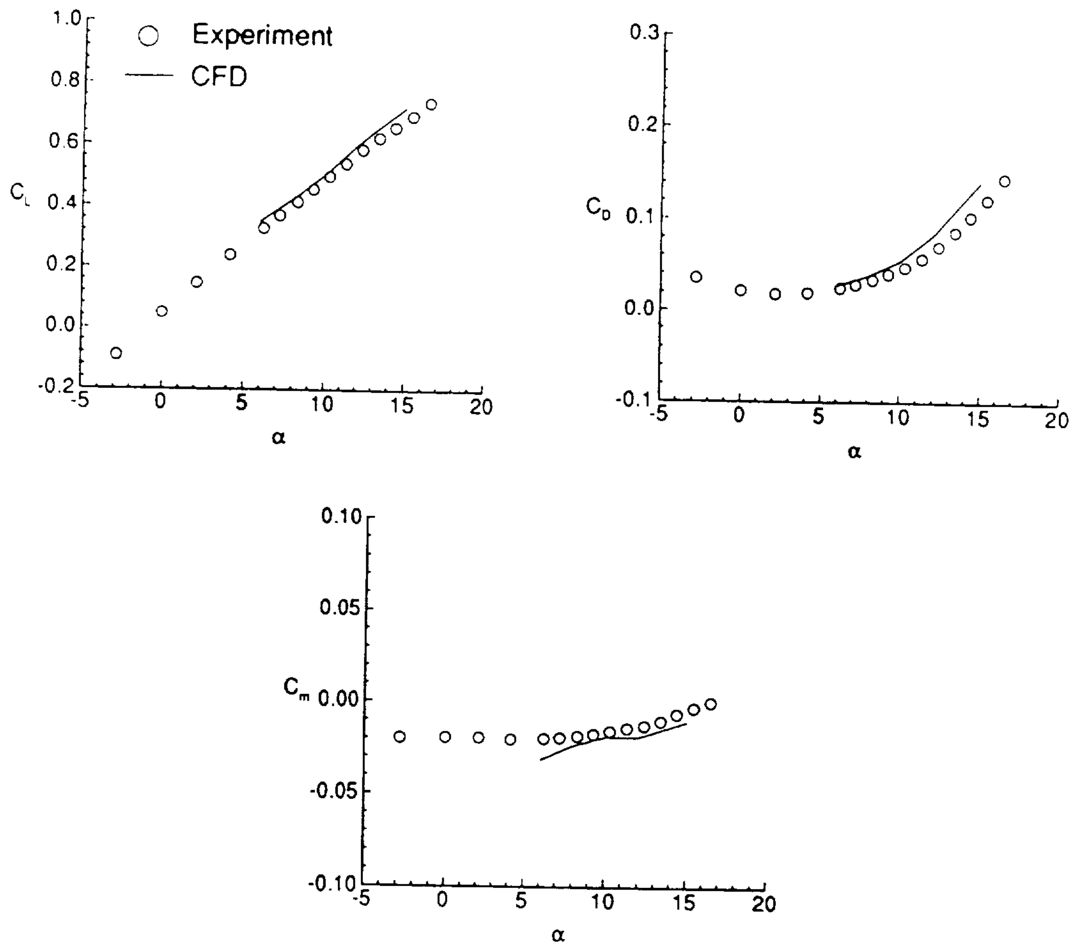

This figure shows the predicted forces and moments compared to experiment for config1, which it the RefH high-lift wing/body configuration. Good correlations are seen, though there is some overprediction of the lift and drag. The pitching moment trend is good but questionable $\alpha = 6°$.

Reference H C_p Comparisons at $\alpha = 6°$

M = 0.24, Re = 8 mil

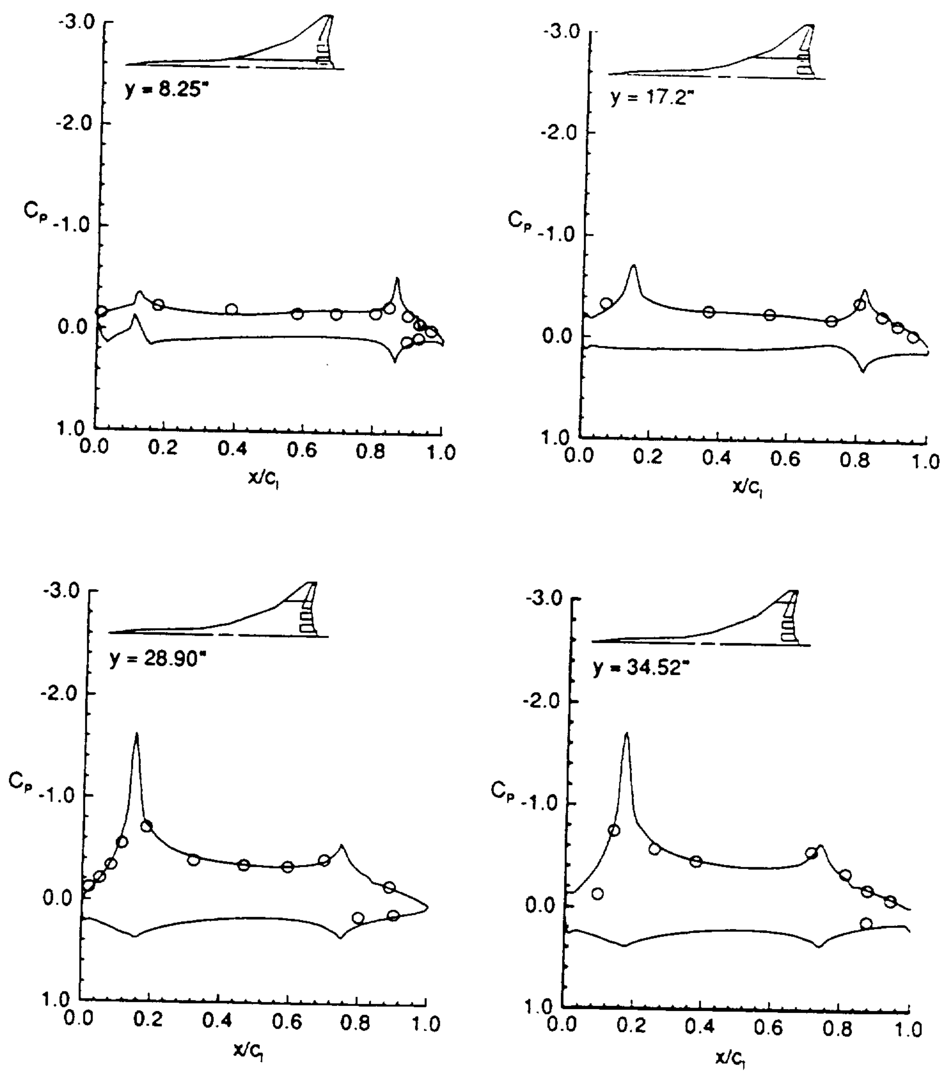

The predicted chordwise pressure distributions extracted from the solution shown on the previous slide are compared to experiment and show very good correlation.

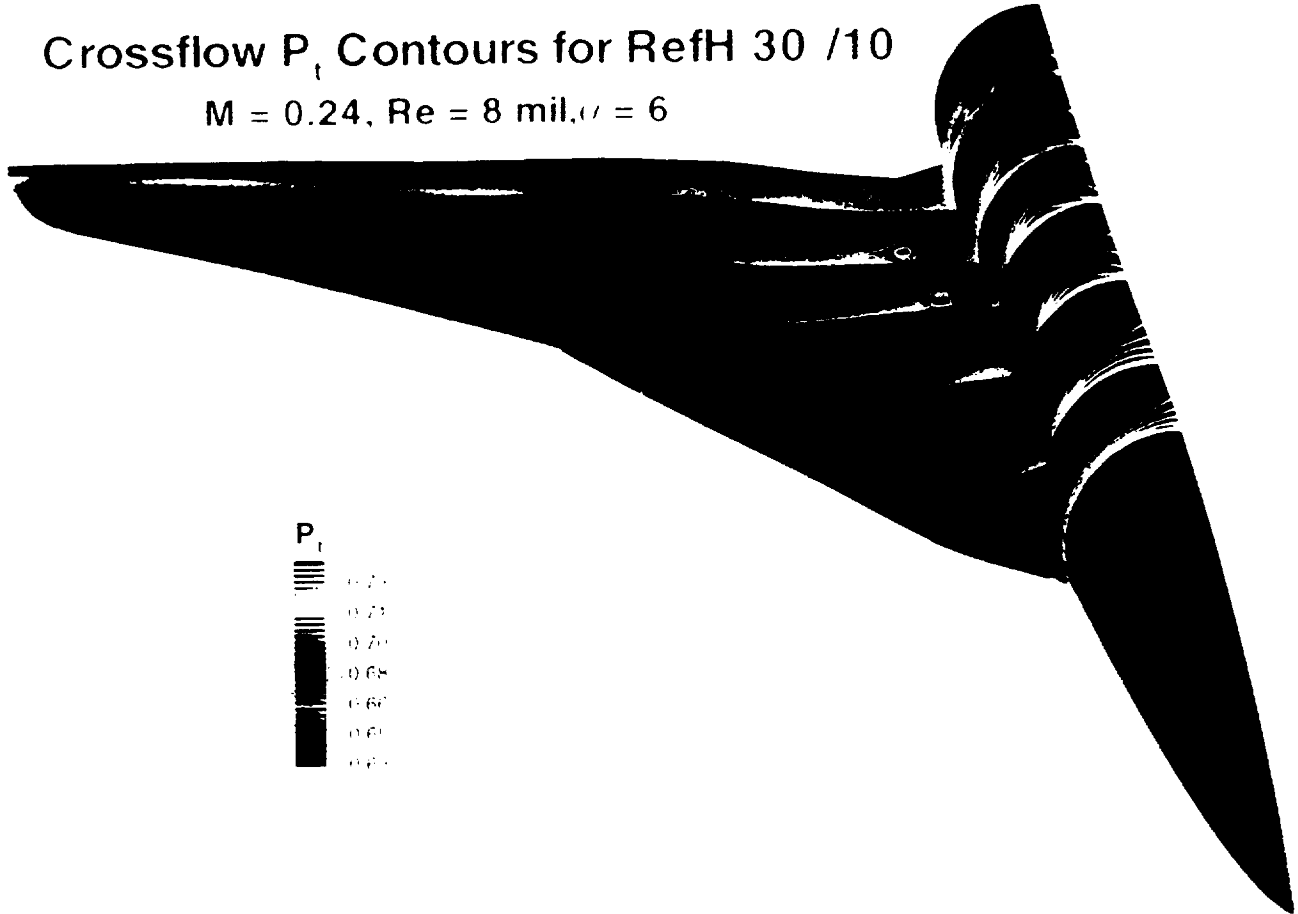

Total pressure contours are plotted in six crossflow planes at $\alpha = 6^\circ$ for the RefH wing/body configuration. In general, the flow on the wing is attached except for a small inboard vortex, which emanates from the apex of the wing.

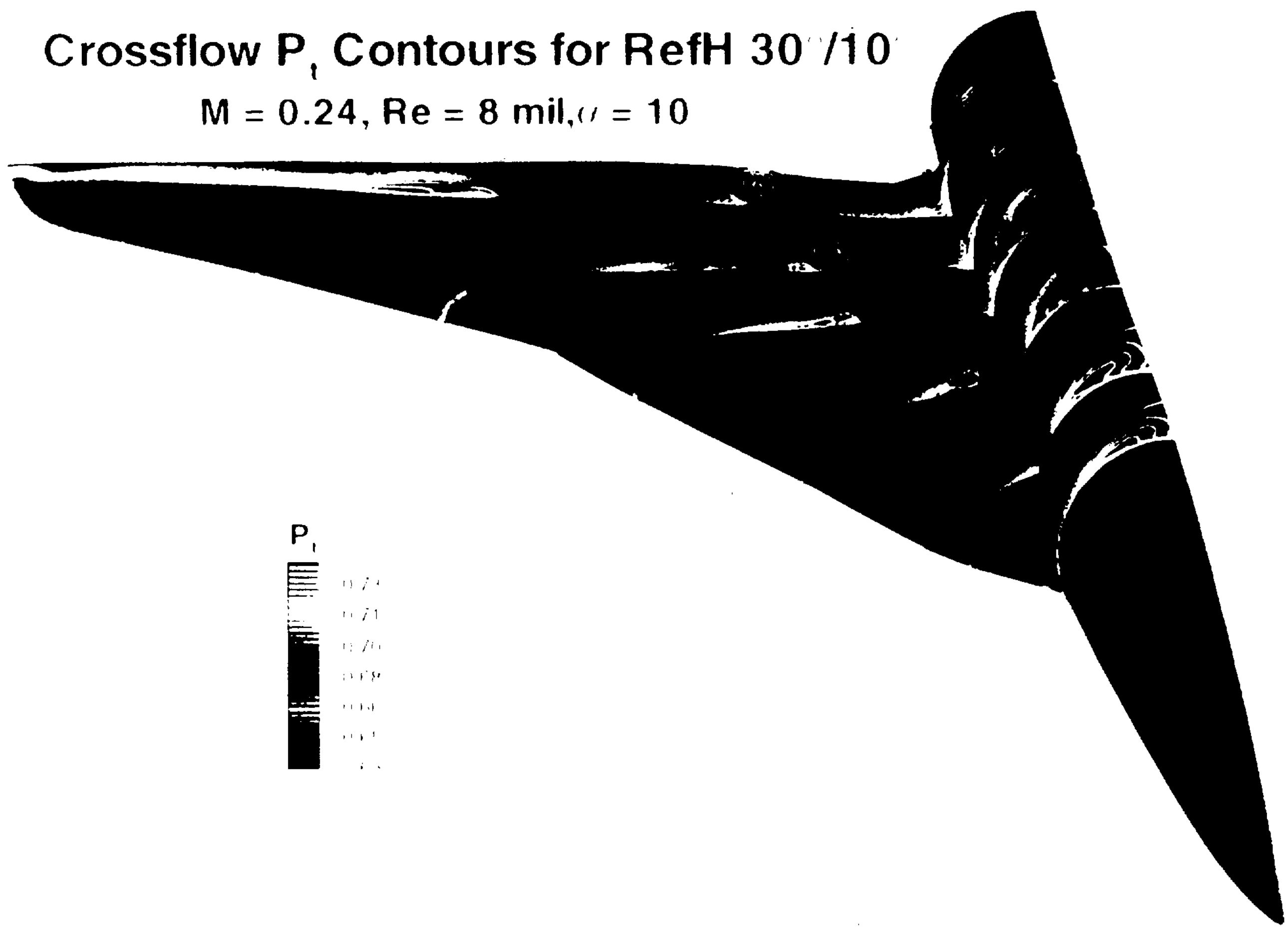

Total pressure contours are plotted in six crossflow planes at $\alpha = 10°$ for the RefH wing/body configuration. Another vortex has formed outboard of the apex vortex, and this elongated vortex emanates from the leading-edge hingeline. A weak crank vortex has developed and appears confined to the leading-edge flap region as it propagates downstream. A fuselage vortex has also formed.

Reference H C_p Comparisons at $\alpha = 10°$

M = 0.24, Re = 8 mil

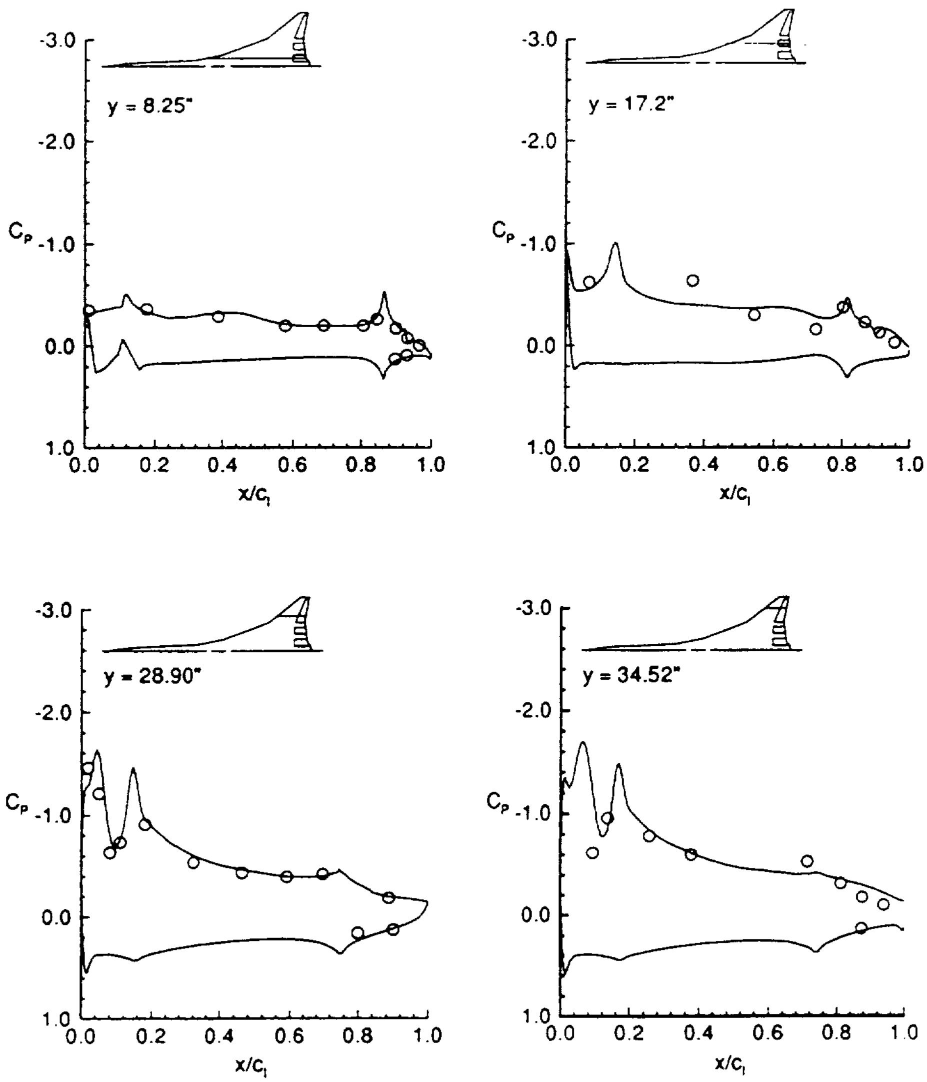

The predicted chordwise pressure distributions extracted from the solution shown on the previous slide are compared to experiment and again show good correlation, though some discrepancies are seen on the trailing-edge flap at y = 34.52"

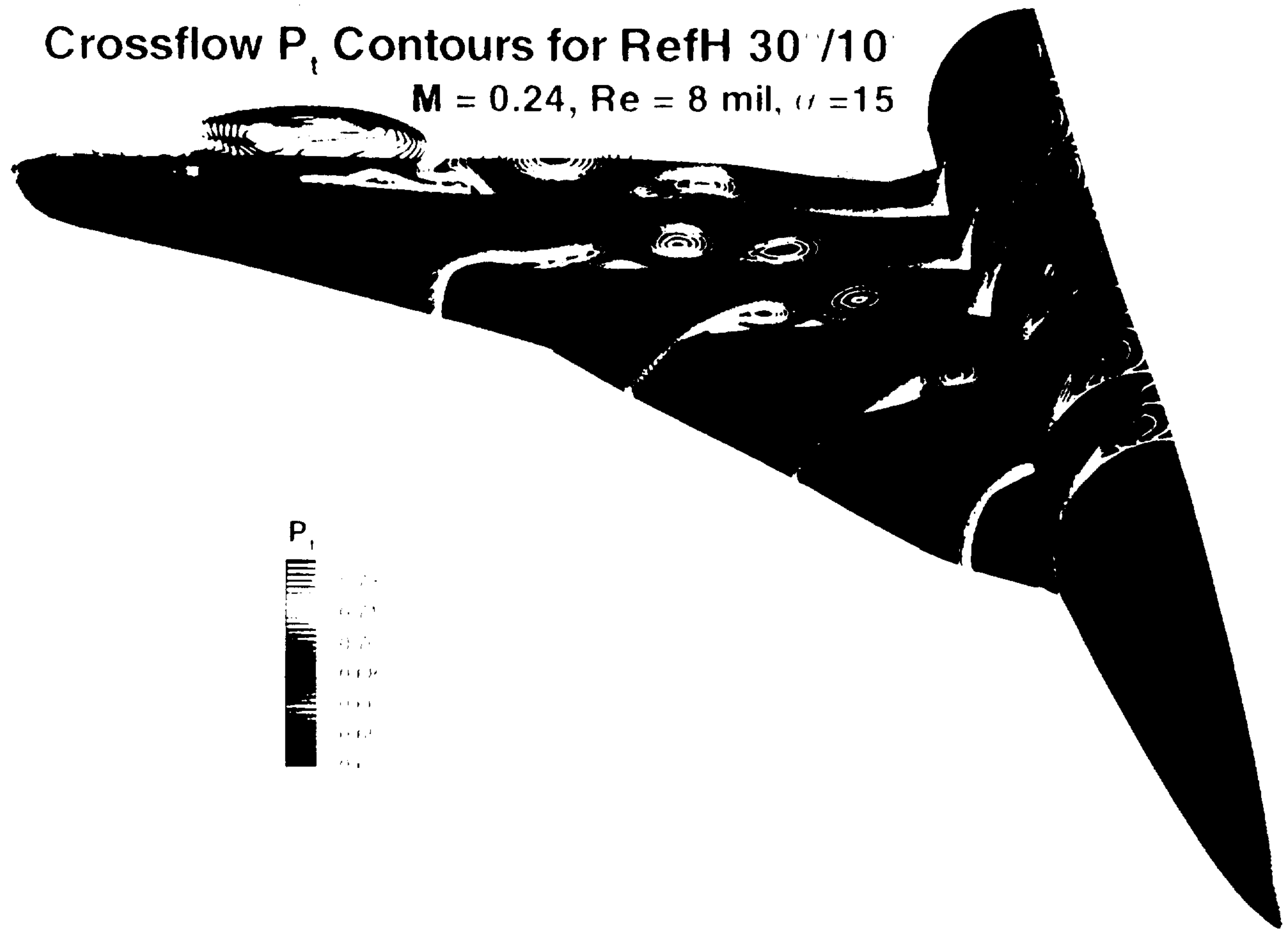

Total pressure contours are plotted in six crossflow planes at $\alpha = 15°$ for the RefH wing/body configuration. A very complicated vortical flow pattern has developed, and all the vortices that were present for the $\alpha = 10°$ case have increased in size and strength. The crank vortex merges with a leading edge vortex which develops just upstream of the crank. This combined vortex moves inboard onto the wing as it travels downstream where it begins to dissipate near the trailing edge.

Reference H C_p Comparisons at $\alpha = 15°$

M = 0.24, Re = 8 mil

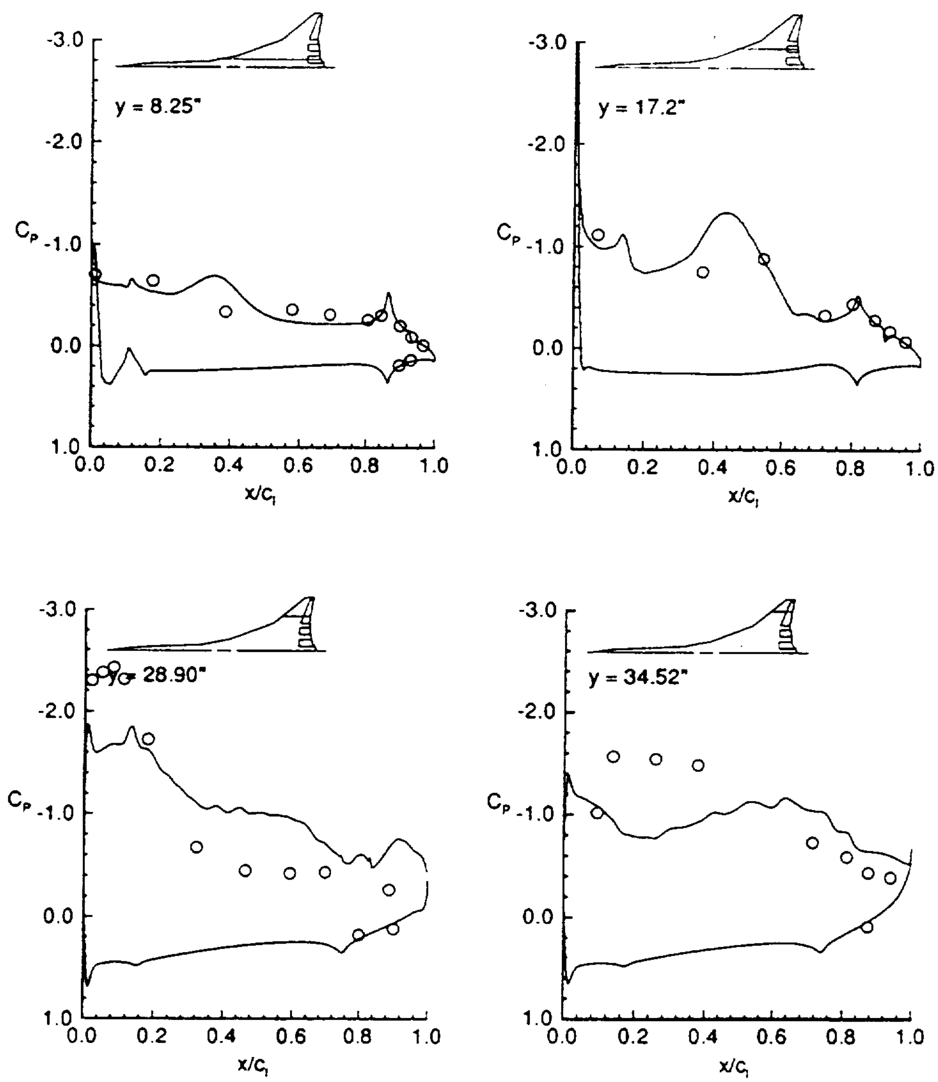

The predicted chordwise pressure distributions extracted from the solution shown on the previous slide are compared to experiment and correlate well for the first two chordwise stations. However due to the massive flow separation on the outboard of the wing, the predicted pressure distributions show poor comparisons. Note in particular the decrease in the predicted suction peak values at the leading-edge.

Forces and Moments for Reference H w/b/nac/htail

M = 0.24, Re = 8 mil

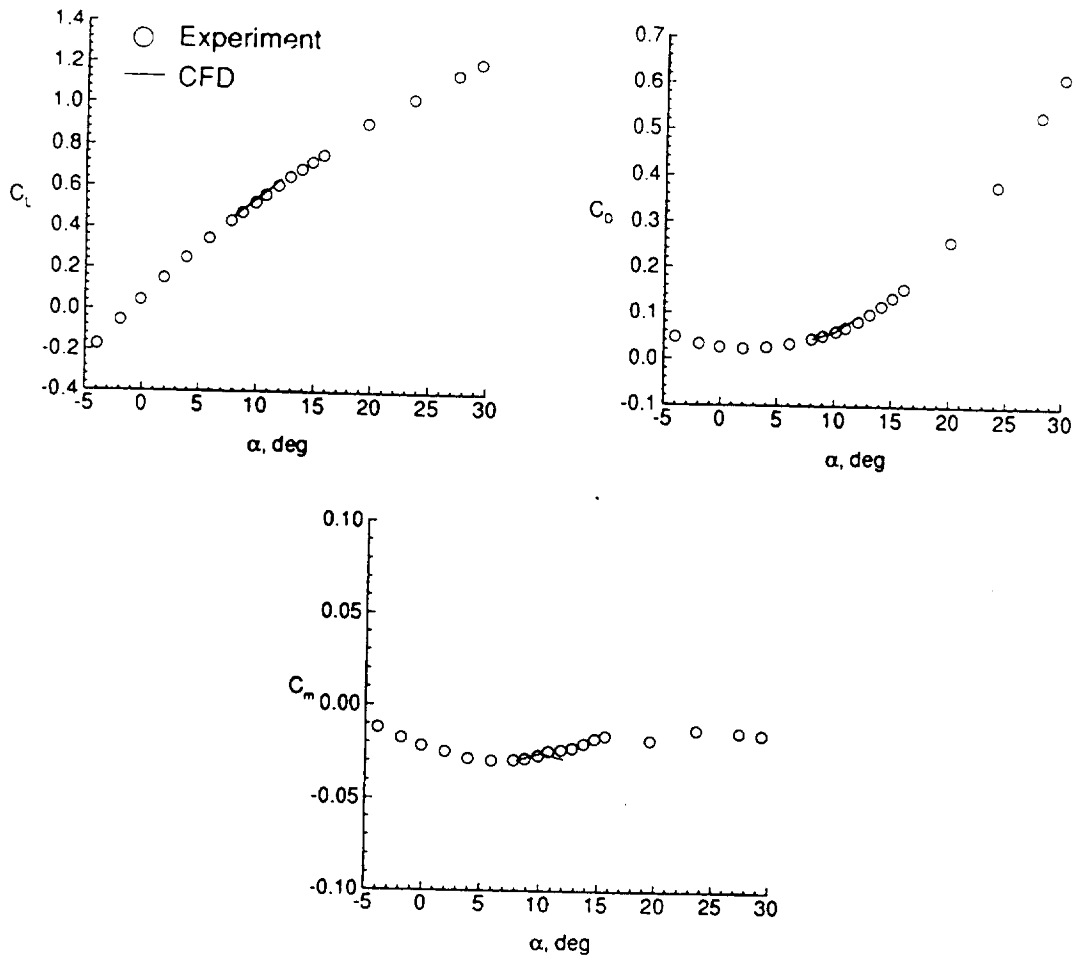

This figure shows the predicted forces and moments compared to experiment for config2, which is the RefH high-lift wing/body/nac/htail configuration. Very good correlations are seen. Since the surface pressure distributions were similar for both config1 and config2, no C_p comparisons are shown for config2. Off-surface contours on the wing were also similar for both cases, though some differences are noted in the wake region.

Full Span RefH 30°/10° Surface Grid

w/b/nac/emp

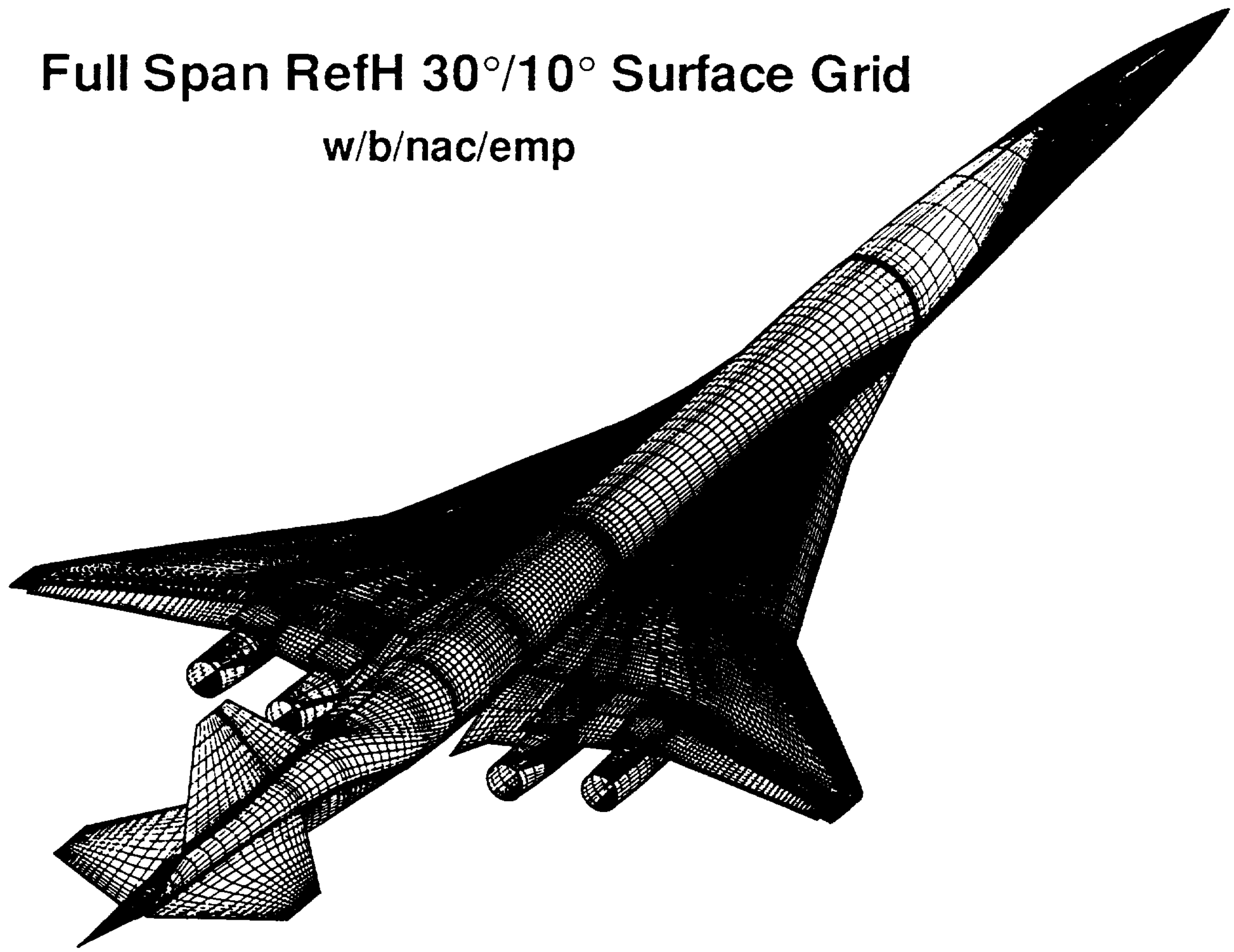

The full-span Reference H (30/10) wing/body/nacelle/empennage surface grid is shown here. This grid contains over 7.0 million points and has 74 blocks. Lateral performance calculations were made using this grid at $\alpha = 8°$, and $\beta = 0°, 6°, 12°$, and $15°$.

Forces and Moments for RefH w/b/nac/emp

M = 0.24, Re = 8 mil

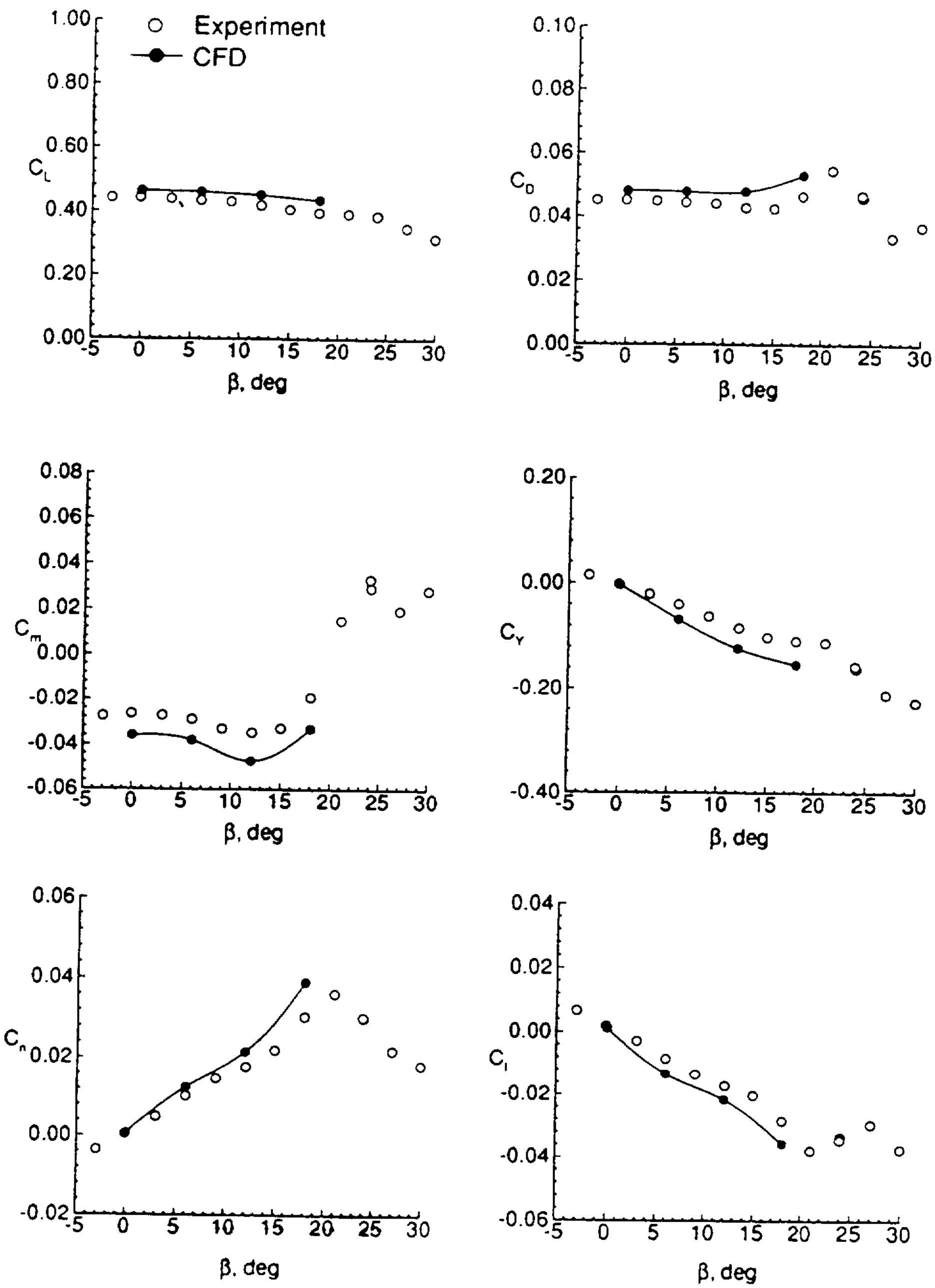

The computed forces and moments for the full-span RefH configuration obtained at a sideslip angle of 12° and at $\alpha = 8°$ are compared to experiment. The lateral performance trends are well predicted, though the point values tend to deviate more than the previous cases. This could be due to the coarseness of the grid.

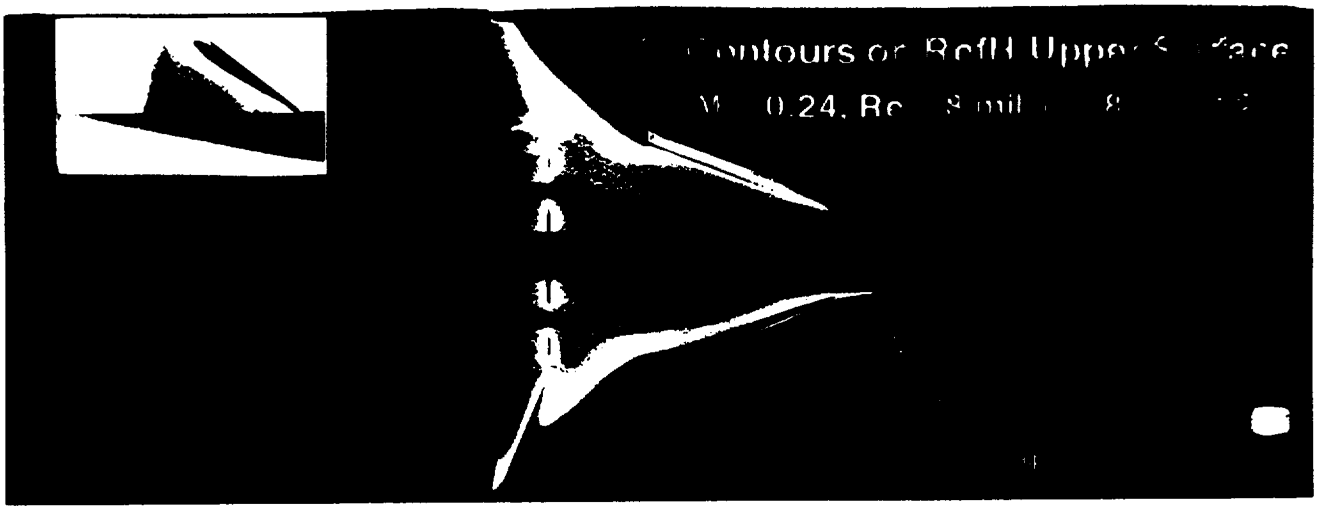

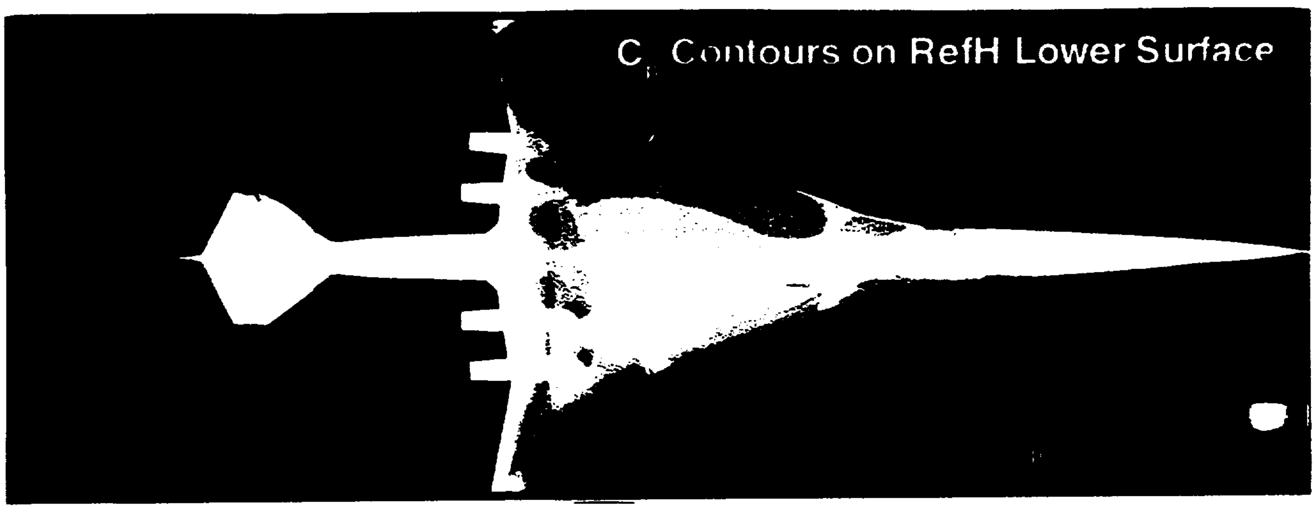

Surface pressure contours for the upper and lower surfaces of the RefH at a 12° sideslip angle are shown. Note the higher loading of the right wing, which is characterized by higher suction peaks compared to the left wing. A vortex has also formed on the leading-edge of the vertical tail.

RefH C_p Comparisons at $\alpha = 8°$, $\beta = 12°$

M = 0.24, Re = 8 mil

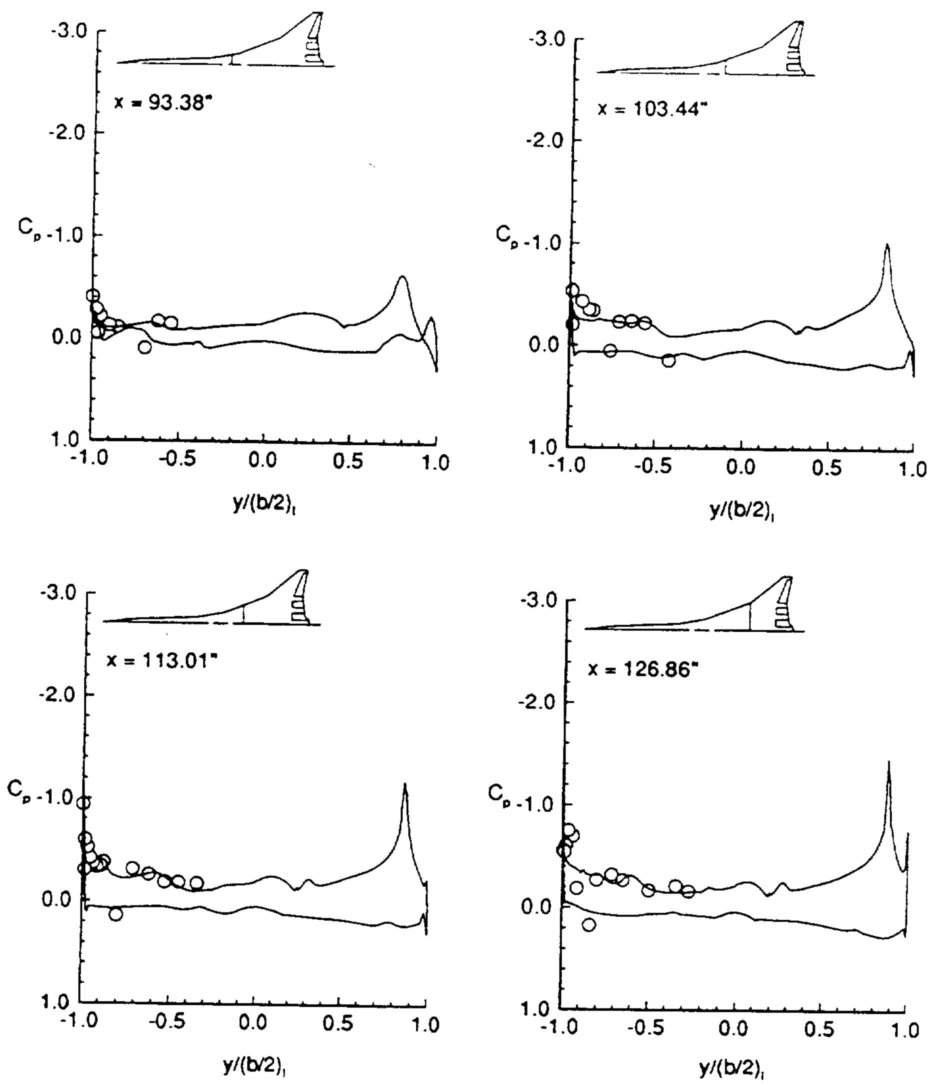

This figure shows C_p comparisons for the full-span configuration at four fuselage stations. The spanwise distance on each plot ranges from -1.0 to +1.0, where the 0 to -1.0 interval represents the left wing and the 0 to +1.0 interval represents the right wing. Note the asymmetry of the pressure distribution curves and the higher suction peaks that occur on the right wing. Correlations are fair and could probably be improved with more grid resolution in the leading edge regions.

RefH C_p Comparisons at $\alpha = 8°$, $\beta = 12°$

M = 0.24, Re = 8 mil

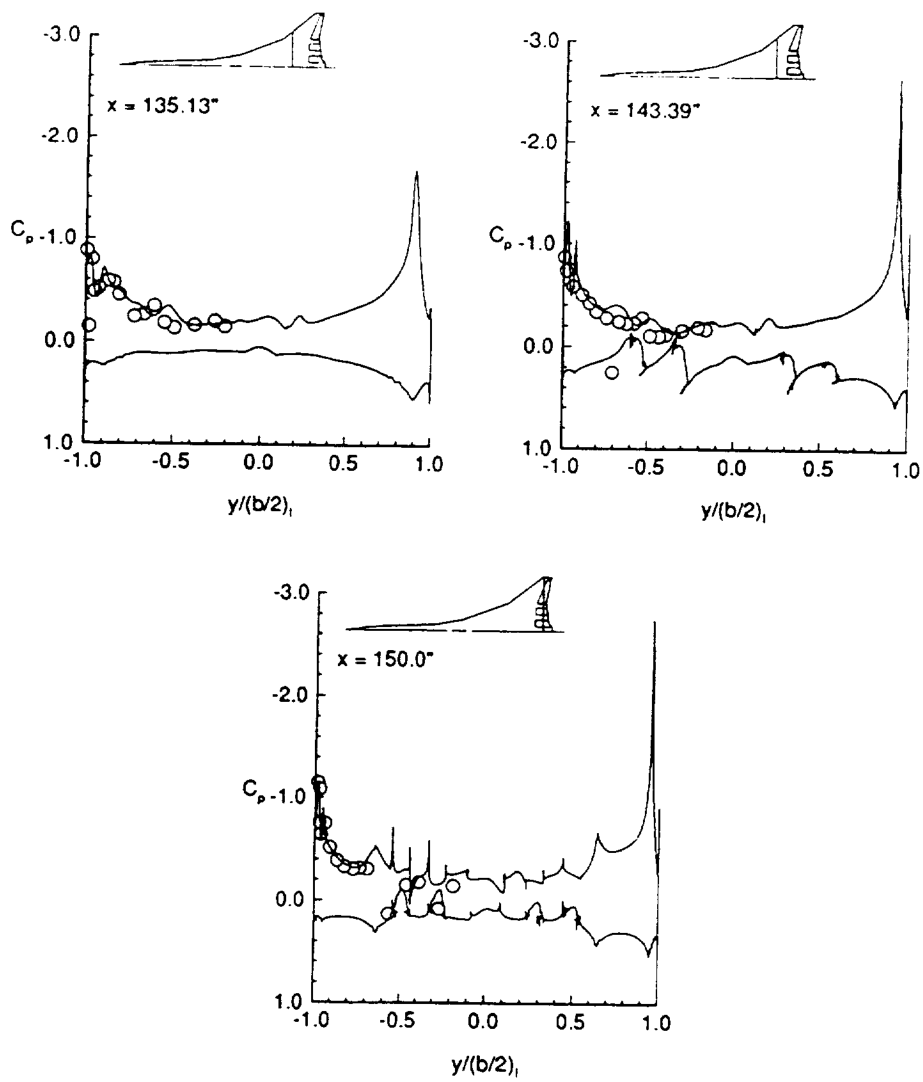

This figure shows C_p comparisons for the full-span configuration at three downstream spanwise stations. Fair to good correlations are noted. The nonsmooth lower surface pressures at x = 143.39" are due to the alternating high pressure, low pressure effects that occur on the nacelles at a 12° sideslip angle. Likewise the choppy pressure distributions depicted at x = 150" were expected since the pressures were extracted on and around the trailing-edge flaps.

RefH C_p Comparisons at $\alpha = 8°$, $\beta = 12°$

M = 0.24, Re = 8 mil

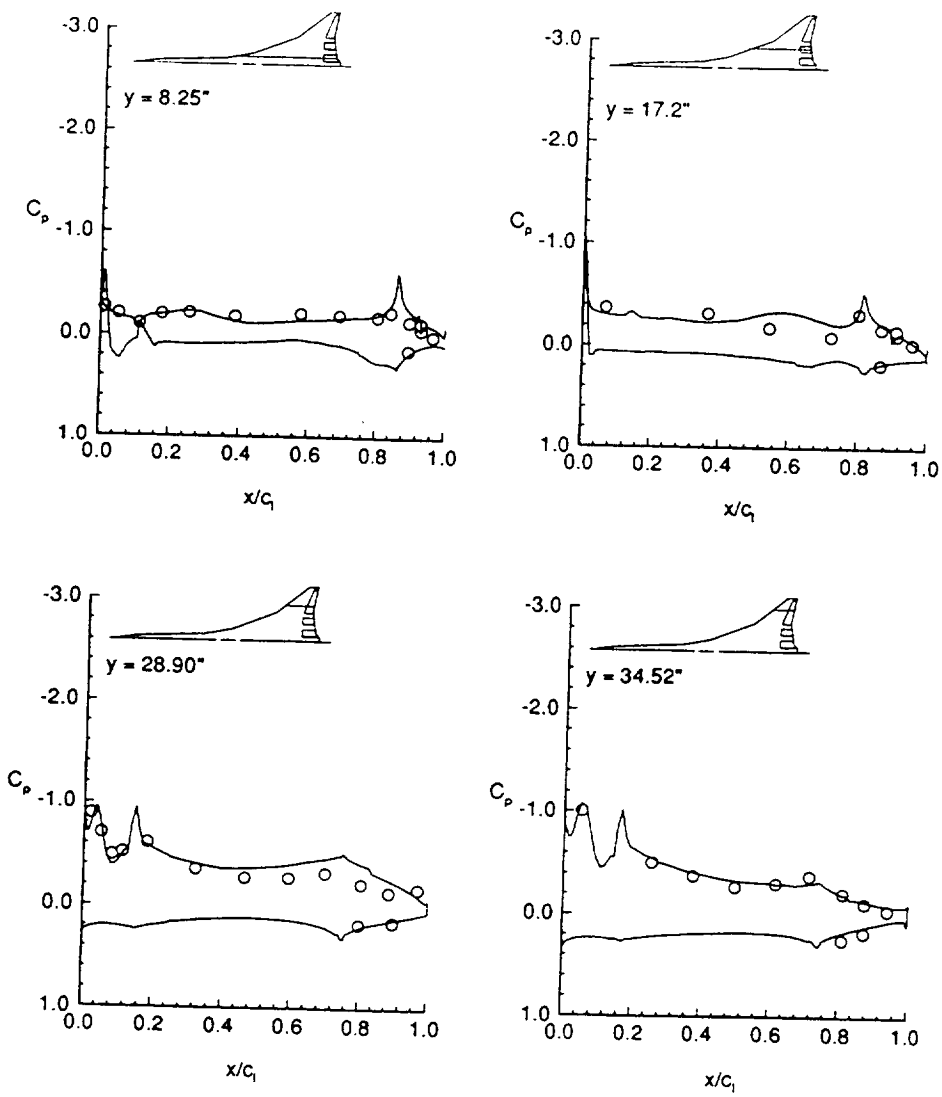

This figure shows C_p comparisons at four chordwise stations and correlation between computation and experiment are good.

Reference H C_p Comparisons with Two Different Grids

M = 0.24, Re = 8 mil, α = 8°, β = 0°

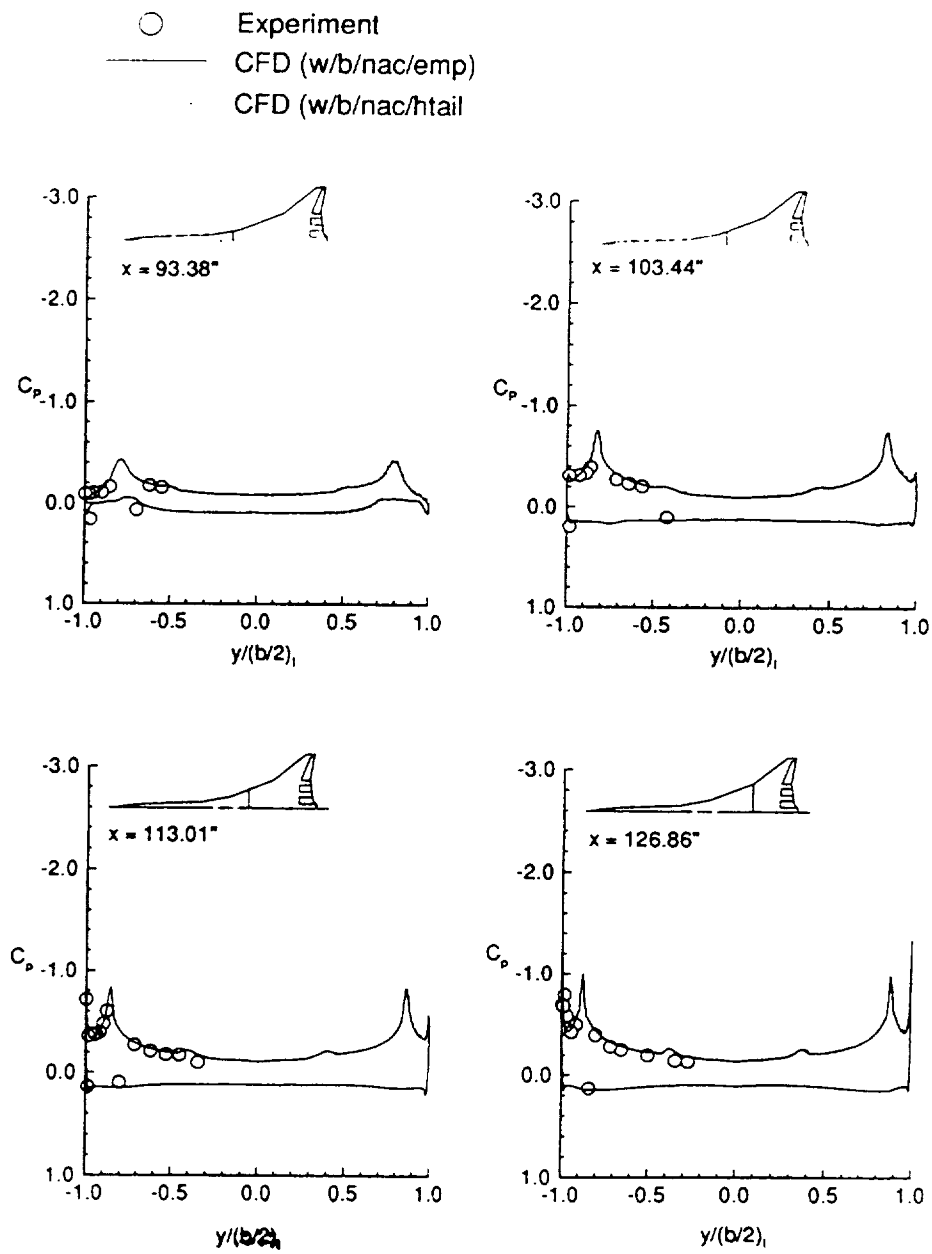

Since the full-span high-lift RefH grid (config3) was a mirrored coarser version of config2, C_p comparisons were made at the various chordwise and spanwise stations to address any grid effects in the sideslip solutions. This figure shows the pressure distributions at four spanwise stations obtained by the two grids; the experimental values are also plotted. Excellent agreement is seen between the two CFD solutions using the different grids, and correlation with experiment is also good.

Reference H C_p Comparisons with Two Different Grids

M = 0.24, Re = 8 mil, $\alpha = 8°$, $\beta = 0°$

Experiment
CFD (w/b/nac/emp)
CFD (w/b/nac/htail)

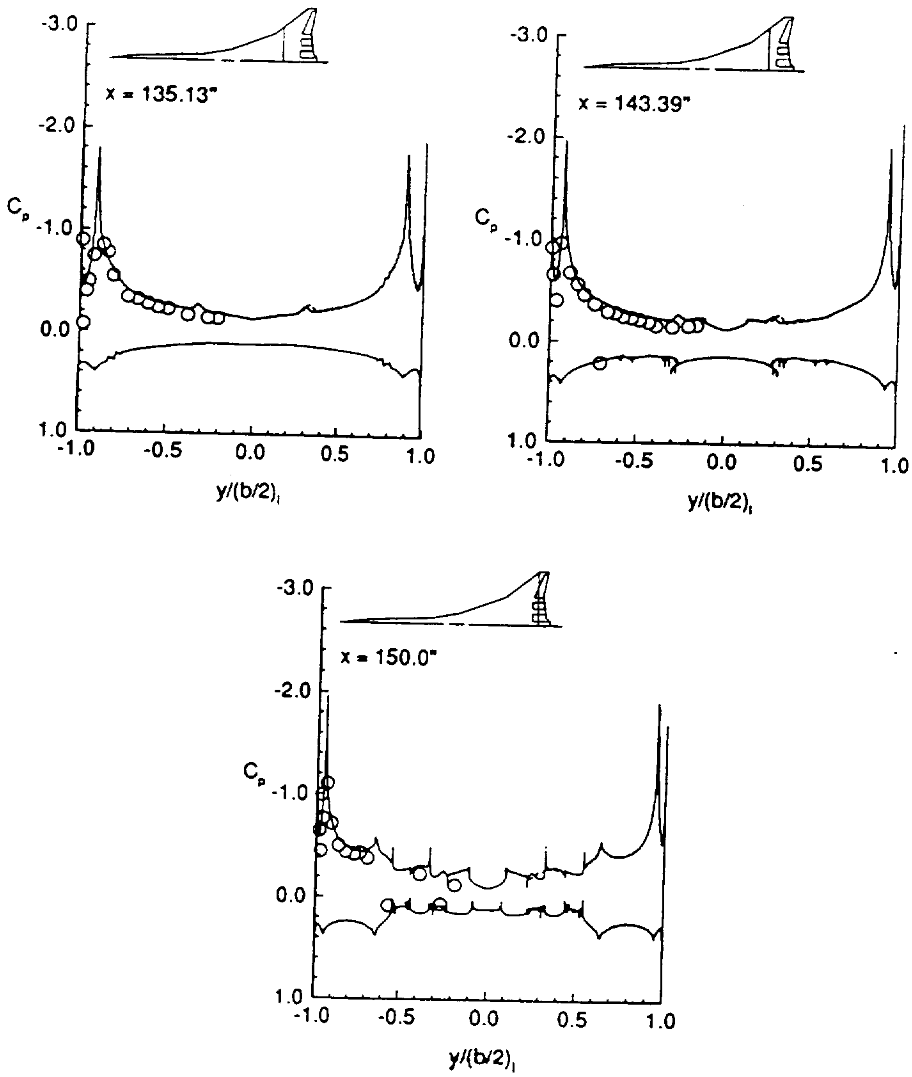

C_p comparisons made at three additional downstream spanwise stations show a slight deviation in pressures at the inboard suction peak at approximately $y/(b/2)_l = 0.40$. Correlaton with experiment shows good agreement.

CONCLUSIONS

- Computational results correlated well with experimental force and moments data and were capable of predicting the longitudinal and lateral performance trends.
- Predicted surface pressures compared well to experiment except when the flow began to develop extensive outboard separation.
- Predicted off-surface and surface flow viz offers insight into the flow physics and continues to provide important details that the wind-tunnel does not.
- Multi-block structured grids for high-lift w/b/nac/emp HSCT configuration is still a time consuming process in terms of grid generation and code set-up/debugging.

HSR H-L CFD

The slide is self-explanatory

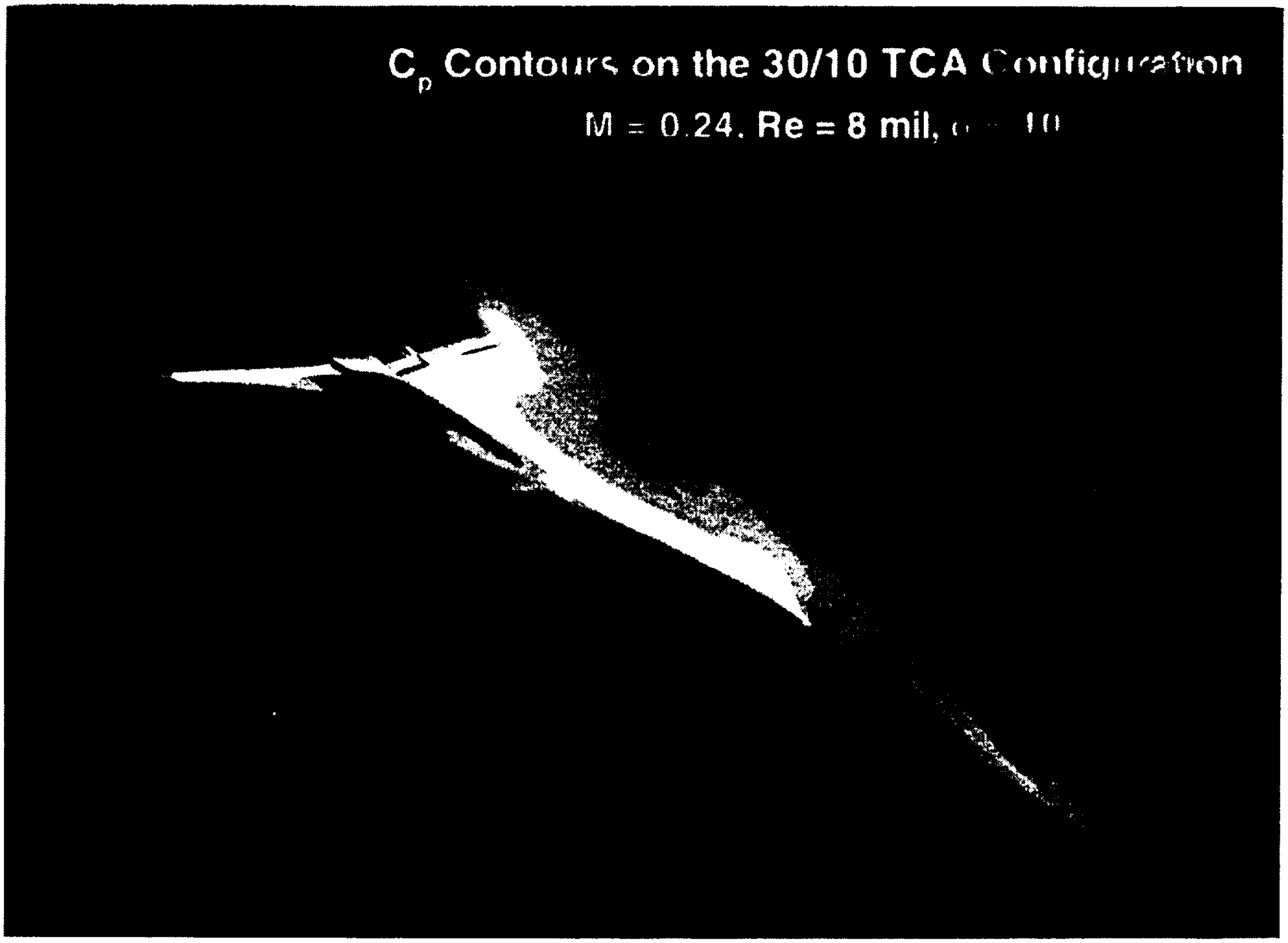

Future work will include solving the high-lift flow about the Technology Concept Airplane (TCA) using CFL3D. Surface pressure contours are shown in this figure at $\alpha = 10^\circ$.

This page intentionally left blank.